Selection Rules for Transport Excitation Spectroscopy of Few-Electron Quantum Dots

Daniela Pfannkuche

Max-Planck-Institut für Festkörperforschung, Heisenbergstrasse 1, D-70569 Stuttgart, Germany

Sergio E. Ulloa

Department of Physics and Astronomy and Condensed Matter and Surface Sciences Program, Ohio University, Athens, Ohio 45701-2979

Tunneling of electrons traversing a few-electron quantum dot is strongly influenced by the Coulomb interaction leading to Coulomb blockade effects and single-electron tunneling. We present calculations which demonstrate that correlations between the electrons cause a strong suppression of most of the energetically allowed tunneling processes involving excited dot states. The excitation of center-of-mass modes, in contrast, is unaffected by the Coulomb interaction. Therefore, channels connected to these modes dominate the excitation spectra in transport measurements.

Transport measurements are a highly sensitive tool for the investigation of the electronic structure of semiconductor quantum dots. While the differential conductance of such a system in the linear transport regime is dominated by the classical Coulomb blockade effect [1], quantum mechanics leaves its fingerprints in magnetic field dependent addition spectra [2,3] and in excitation spectra which can be obtained from conductance measurements in the finite drain-source voltage regime [4–6].

Because of a small electronic effective mass, quantum dots in semiconductor heterostructures exhibit a discrete level spectrum, easily discernible at low temperatures. Since the charge of these quantum dots can be controlled at the single-electron level, they are often called *artificial atoms*. The lateral confinement potential which binds the electrons to the quantum dot is typically created by spatially extended charge distributions. Therefore, it obeys a parabolic dependence on the distance from the center of the system ($\propto r^2$) rather than the $1/r$ dependence characteristic of the core potential of *natural* atoms [7]. In analogy to the optical spectroscopy on conventional atoms the first attempts to study the excitation spectrum of these artificial atoms have been made by far-infrared (FIR) spectroscopy [8–11]. However, the long wavelength of the far-infrared radiation together with the parabolic confinement potential prohibit most transitions into excited states by strict dipole selection rules [12,13].

Transport spectroscopy, on the other hand, is expected not to suffer from these restrictions, but to allow a unique full spectroscopy of the level structure in these artificial atoms. Nevertheless, experiments on few-electron quantum dots exhibit only a sparse excitation spectrum with relatively large level spacings [5]. These measurements suggest that the dominant resonances are due to a constant level spacing, independent of the number of electrons in the quantum dot. This behavior, which could be understood for a noninteracting electron system, is indeed remarkable, since the Coulomb interaction strongly influences the energy spectrum of the quantum dot and leads to small level spacings and strong correlations [12,14].

Thus, the experimentally observed large level spacing together with the appearance of a characteristic excitation energy demand an explanation. We present calculations which show that even in transport experiments the excitation spectra are dominated by center-of-mass modes, similar to the situation in FIR spectroscopy. This gives rise to the constant level spacing with the characteristic single-particle excitation energy. This situation is caused by a suppression of most other transitions due to strong *correlations* between the electrons.

We study the transport properties of a two-dimensional quantum dot coupled to two reservoirs by tunneling barriers in the conventional tunneling Hamiltonian approach [15]. The Hamiltonian of the system is given by a sum of the dot Hamiltonian H_D, a reservoir Hamiltonian H_R, and a tunneling term H_T. The tunneling Hamiltonian describes the transfer of electrons from the reservoir, where the Coulomb interaction between the electrons is effectively screened (metallic regime), to the quantum dot, where interactions are most important. Our results are based on features of the few-particle eigenstates of the quantum dot which we obtain from a numerical diagonalization of the dot Hamilton operator

$$H_D = \sum_n \epsilon_n d_n^\dagger d_n + \sum_{n,m,n',m'} V_{nmn'm'} d_n^\dagger d_m^\dagger d_{n'} d_{m'}. \quad (1)$$

It describes interacting electrons in a parabolic confinement potential subjected to a perpendicular magnetic field B. The single-particle energies ϵ_n are connected with left and right circularly polarized oscillator eigenmodes,

$$\epsilon_n = \hbar\Omega_+(N_+ + 1/2) + \hbar\Omega_-(N_- + 1/2), \quad (2)$$

with $\Omega_\pm = (\sqrt{4\Omega_0^2 + \omega_c^2} \pm \omega_c)/2$. Ω_0 characterizes the confining potential and $\omega_c = eB/mc$ is the cyclotron frequency. A crucial feature of the parabolic confinement

potential is the separation of the dot Hamiltonian into a relative and a center-of-mass (CM) part [16,17], where the spectrum of the CM Hamiltonian is identical to the single-particle spectrum (2) and independent of the number of electrons in the dot. It is this separation which prohibits in FIR spectroscopy the observation of the spectral fine structure of these artificial atoms, and makes visible only the CM excitations. The Coulomb interaction between electrons enters only the Hamiltonian of the internal degrees of freedom (relative part). We obtain the matrix elements for the interaction $V_{nmn'm'}$ in closed form for the usual $1/\varepsilon r$ Coulomb potential with the dielectric constant ε.

Regarding only sequential tunneling, the current through the quantum dot is given by [15]

$$I = -e \sum_{\alpha,\alpha'} \Gamma_{\alpha\alpha'}[P(N,\alpha) + P(N-1,\alpha')]$$
$$\times [f(\Delta E_{\alpha\alpha'} - \mu_l) - f(\Delta E_{\alpha\alpha'} - \mu_r)], \quad (3)$$

where the resonant energy $\Delta E_{\alpha,\alpha'} = E(N,\alpha) - E(N-1,\alpha')$ is the difference between the energy of an N-particle state α and an $(N-1)$-particle state α'. The Fermi-Dirac distribution function f characterizes the occupation of electron levels in the left (electrochemical potential μ_l) and the right (μ_r) reservoir. The probability $P(N,\alpha)$ of finding the quantum dot in the N-particle state α will deviate from its equilibrium value for a given drain-source voltage $(\mu_l - \mu_r)/e$. Its dependence on the tunneling rate $\Gamma_{\alpha\alpha'}$ is well described by kinetic equations [15,18] and leads to the blocking of conducting channels and negative differential conductance [5,15,19].

In a "random phase" approximation, i.e., neglecting phase correlations between the initial state of the electron in the lead and its final state in the quantum dot, the tunneling rate $\Gamma_{\alpha\alpha'}$ factorizes into an effective tunneling rate for a noninteracting electron traversing the barrier, γ, and an overlap or spectral weight matrix element [15]. (For simplicity, we assume a constant effective tunneling rate and neglect the dependence of γ on the single-electron dot states.) The overlap matrix element is given by

$$\sum_n |\langle N,\alpha|d_n^\dagger|(N-1),\alpha'\rangle|^2. \quad (4)$$

This quantity describes to what extent the compound state, built by an incoming electron and the $(N-1)$-electron state α' in the dot, overlaps with the N-electron dot state α. While for an uncorrelated electron system this overlap evaluates to unity, correlations reduce it considerably [15,20]. Because of the summation over all single-particle dot states with equal weight in Eq. (4) this quantity is insensitive to any features of the incoming electron. It only reflects the correlations in the states α and α'. In the following we will concentrate on these overlap matrix elements, as they predominantly determine the transport through the quantum dot (for levels separated by more than kT, as discussed, for example, in Ref. [15]; in experiments, $kT \approx 50$ mK ≈ 4 μeV). Our

numerical results are obtained for quantum dots with up to $N = 3$ electrons.

Figure 1 shows the spectra of a quantum dot (QD) occupied by one, two, or three electrons (QD hydrogen, QD helium, or QD lithium) at zero magnetic field. Because of the Coulomb interaction the level spacing of the few-particle spectra is much smaller than the single-electron level spacing, which is given by the confining energy $\hbar\Omega_0 = 2$ meV (this value is characteristic of experimental geometries, such as the system in Ref. [5]). Enforced by energy conservation, tunneling through the quantum dot is only allowed when the energy of the incoming particle matches the energy difference between a QD helium (lithium) eigenstate and a QD hydrogen (helium) eigenstate. The occurrence of all energetically allowed transitions would clearly result in a dense excitation spectrum. That contradicts recent experiments [5]. Thus, it is not only the energy requirement which determines whether an electron tunnels through the quantum dot. A mechanism to select certain transitions is provided by the overlap matrix elements, Eq. (4).

One of these selection rules is evident from spin conservation [19]. For our few-electron quantum dots they forbid transitions between a spin singlet state of QD helium and a spin quartet state of QD lithium. This already has consequences for the usual Coulomb blockade oscillations, as transitions between the ground states of QD helium and QD lithium (G-G transition) in a perpendicularly applied magnetic field are considered. The total spin of
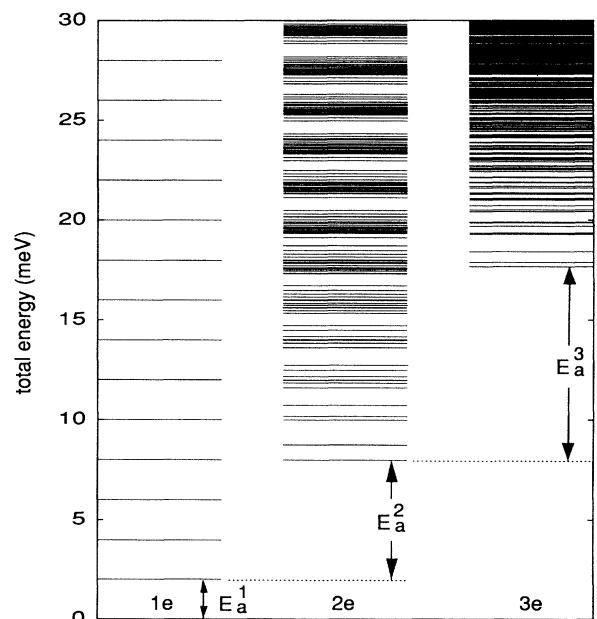

FIG. 1. Level scheme of a parabolic quantum dot with one, two, or three electrons at $B = 0$ T. Arrows represent the corresponding addition energies. Parameters for all figures: confining energy $\Omega_0 = 2$ meV; GaAs parameters: dielectric constant $\varepsilon = 12.4$, effective mass $m^* = 0.067m_e$.

the ground state of these few-electron systems oscillates between its maximum (triplet, respectively, quartet) and its minimum value (singlet, respectively, doublet), when the magnetic field is increased [16,17]. Figure 2 shows the ground state energy of QD helium and QD lithium as a function of the magnetic field B. The total spin is indicated for the different field ranges. For most values of the magnetic field G-G transitions are possible. However, as indicated in the figure, two field ranges occur where the ground state of QD helium is a singlet while that of QD lithium is a quartet: the G-G transition is blocked. Thus, a drastic reduction of the conductance in the linear response regime should be observed when the magnetic field is tuned into these ranges.

However, spin selection rules alone are not sufficient to explain the sparseness of the observed excitation spectra. Apart from an angular momentum conservation in the dot, the effect of which is annihilated by connecting the dot laterally to the leads, the overlap matrix elements, Eq. (4), provide no further strict selection rules. Nevertheless, very small spectral weights strongly reduce the probability for the occurrence of the corresponding transitions. This gives rise to *quasiselection rules*. Figure 3 shows the values of the overlap matrix elements for transitions from the QD-helium ground state to all states of QD lithium at $B = 0$. They correspond to the most important processes, if the quantum dot is in its ground state before the subsequent tunneling process. Since the two-particle ground state is a singlet state, only transitions into doublet states are possible. Transitions into degenerate states are subsumed under the same peak, since all corresponding overlap elements contribute accordingly to the tunneling rate at a given energy ΔE. This applies especially to

the double degeneracy with respect to the z component of the doublet spin, giving rise to a factor of 2 in the peak heights. At low energies, below 15 meV, the figure exhibits a few regularly spaced dominant peaks with several relatively smaller ones between them. This energy regime coincides with the experimental situation where only one electron tunnels at a time [5].

The first peak at 9.7 meV corresponds to the G-G transition. The $B = 0$ states are, apart from the spin degeneracy, degenerate with respect to the sign of the angular momentum. Therefore, the three-particle ground state (with an orbital angular momentum of $\hbar$) is fourfold degenerate. Each of these states contributes equally to the peak shown in Fig. 3. Thus, the individual overlap matrix elements [Eq. (4)] are much smaller than unity, indicating the strong correlations in the few-particle states. Nevertheless, compared with the other spectral weights the individual overlap matrix elements of the G-G transition are the largest. Therefore, these transitions occur with the highest probability. They are followed by a transition which is subsumed in the peak appearing at 11.7 meV, i.e., at an excitation energy of 2 meV $= \hbar\Omega_0$ above the G-G transition. This transition corresponds to a state of the three-particle system with one quantum of CM excitation in addition to the ground state energy. As a consequence of the separation of the CM and relative motions, each transition within the internal degrees of freedom is accompanied by independent excitations of CM modes. Since the excitation spectrum of the CM motion is equidistant, these transitions give rise to equidistant conductance peak replicas (see arrows in Fig. 3). Moreover, at zero magnetic field the CM energy spectrum is highly degenerate. Therefore, the overlap matrix elements of several transitions contribute to the tunneling probability for a given resonant energy. It is this prevalence of the CM excitations which provides an expla-
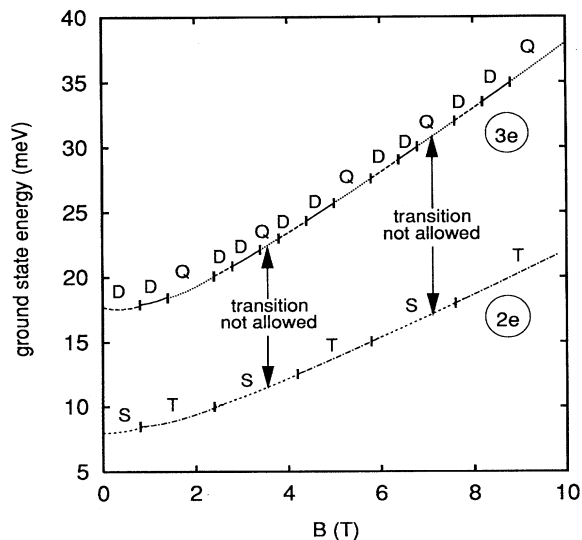

FIG. 2. Ground state energy of a parabolic quantum dot with two and three electrons as a function of the magnetic field B. Spin states are indicated: $S =$ singlet, $T =$ triplet, $D =$ doublet, and $Q =$ quartet. Arrows mark those field ranges where G-G transitions are forbidden by spin selection rules.
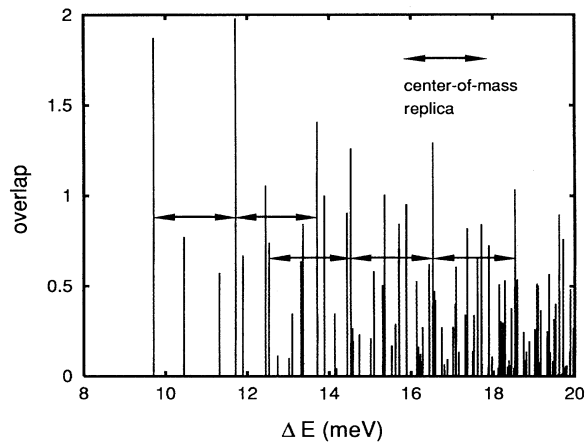

FIG. 3. Summed values of the overlap matrix elements for transitions between the two-particle ground state in the quantum dot at $B = 0$ and all states of the three-electron system as a function of the transition energy ΔE. Arrows indicate center-of-mass excitations.

nation for the experimental observation of a characteristic level spacing independent of the number of particles in the quantum dot: The CM spectrum is independent of the number of particles in a parabolic quantum dot and equals the single-electron spectrum [12]. (Notice that the small thermal broadening of the Fermi level in experiments, typically 100 mK, will not blur the different CM excitations, occurring with much larger spacings, 2 meV here.)

It is clear that in addition to the G-G transition tunneling via other internal excitation states is possible, with their corresponding CM excitation replicas (see second pair of replicas in Fig. 3). In some cases (e.g., in the transition from the single-particle ground state to the first-excited two-particle state, not shown here) the overlap matrix elements can even be larger than those of the G-G transition. Because of their large degeneracy, transitions which end in a maximum-spin state produce very pronounced series of replicas, much stronger than the ones shown in Fig. 3. The occurrence of more than one group of dominant replicas gives rise to smaller level spacings in the spectra. Both effects have been observed in experiment for different N states in the dot. However, we found in all cases that only few groups of dominant replica occurred, while most excitations of internal degrees of freedom *are suppressed in tunneling*. In our model, with a constant tunneling rate γ, this suppression is solely due to correlations of the few-particle wave functions. These strong built-in correlation effects lead to nearly forbidden transitions. Notice that the effective suppression of internally excited states becomes less pronounced in the high energy range, as indicated by a more even distribution of high-overlap peaks in Fig. 3.

Although our calculations only include systems with up to three electrons, general conclusions can be drawn for quantum dots occupied by more electrons. As long as correlations strongly influence the low energy excitations, a strong reduction of most overlap matrix elements occurs, leading to quasiselection rules. These will suppress most transitions involving excitations of the internal degrees of freedom in the rather dense spectrum. Since the CM motion remains unaffected, these degrees of freedom can be excited easily. Thus, it can be expected that they would likewise dominate the transport resonances. Another aspect enhancing the effect of dominant CM excitations may arise especially in large quantum dots laterally connected to the reservoirs by split gate tunnel barriers. This geometry forces the electron to enter at a certain point at the edge of the dot. This introduces a large dynamical dipole moment in the system built out of the incoming electron and the $(N - 1)$-particle state in the dot. As known from far-infrared investigations, CM excitations give rise to a strong dipole moment. Therefore, one would expect that the overlap of such a compound state with a CM excitation will be larger than others, thus favoring it for tunneling.

A basic assumption for the discussion so far has been the strict separation of CM and relative motions which is only fulfilled in a truly parabolic confinement potential. How-

ever, calculations which take into account anharmonicities of the confining potential [21] have shown that for realistic conditions [22] the coupling between the CM motion and the relative motion is weak, leaving the demonstrated mechanism for dominant CM excitations essentially unchanged.

In summary, the analysis of the overlap matrix elements which govern the tunneling rate for an electron traveling through a quantum dot shows that the strong correlations present in few-electron dot states are extremely important. They strongly reduce the probability of tunneling through channels involving excitations of the internal degrees of freedom. This leads to a dominance of the center-of-mass excitations which are not affected by correlation effects. The center-of-mass excitation spectrum is identical with the single-particle spectrum of an electron in the parabolic quantum dot, independent of the number of particles. These features give an explanation for the experimental observations in the nonlinear, single-electron tunneling regime, showing relatively sparse excitation spectra with the characteristic single-electron level spacing.

[1] H. van Houten *et al.*, in *Single Charge Tunneling*, edited by H. Grabert and M. Devoret (Plenum Press, New York and London, 1992), p. 167.

[2] P. L. McEuen *et al.*, Phys. Rev. Lett. **66**, 1926 (1991).

[3] R. C. Ashoori *et al.*, Phys. Rev. Lett. **71**, 613 (1993).

[4] A. T. Johnson *et al.*, Phys. Rev. Lett. **69**, 1592 (1992).

[5] J. Weis *et al.*, Phys. Rev. Lett. **71**, 4019 (1993).

[6] E. B. Foxman *et al.*, Phys. Rev. B **47**, 10020 (1993).

[7] A. Kumar *et al.*, Phys. Rev. B **42**, 5166 (1990).

[8] C. Sikorski and U. Merkt, Phys. Rev. Lett. **62**, 2164 (1989).

[9] T. Demel *et al.*, Phys. Rev. Lett. **64**, 788 (1990).

[10] A. Lorke *et al.*, Phys. Rev. Lett. **64**, 2559 (1990).

[11] B. Meurer *et al.*, Phys. Rev. Lett. **68**, 1371 (1992).

[12] P. A. Maksym and T. Chakraborty, Phys. Rev. Lett. **65**, 108 (1990).

[13] Q. P. Li *et al.*, Phys. Rev. B **43**, 5151 (1991).

[14] D. Pfannkuche *et al.*, Phys. Rev. B **47**, 2244 (1993).

[15] J. M. Kinaret *et al.*, Phys. Rev. B **46**, 4681 (1992).

[16] M. Wagner *et al.*, Phys. Rev. B **45**, 1951 (1992).

[17] P. Hawrylak and D. Pfannkuche, Phys. Rev. Lett. **70**, 485 (1993).

[18] C. W. J. Beenakker, Phys. Rev. B **44**, 1646 (1991).

[19] D. Weinmann *et al.*, Europhys. Lett. **26**, 467 (1994).

[20] J. J. Palacios *et al.*, Europhys. Lett. **23**, 495 (1993).

[21] D. Pfannkuche and R. R. Gerhardts, Phys. Rev. B **44**, 13132 (1991).

[22] K. Lier and R. R. Gerhardts, Phys. Rev. B **48**, 14416 (1993).